Ontario Hydro

RESEARCH DIVISION

91602
new 82-10

COMPLIMENTARY COPY
Please Credit Ontario Hydro Research if
Reproduced in Whole or in Part

ontario hydro
research division

PHOTOIONIZATION SCHEMES FOR ATOMIC VAPOUR LASER ISOTOPE SEPARATION OF ZIRCONIUM

Hugh D. Morrison
Engineering Physicist
Science Section
Electrical Research Department

ABSTRACT

Photoionization, the process of ionizing atoms by the absorption of light, is the second of three stages in atomic vapour laser isotope separation (AVLIS) of zirconium. A study of the atomic spectroscopy of zirconium reveals several schemes that may prove useful for photoionizing ^{91}Zr, the isotope to be depleted in the zirconium product. The source of light for these schemes would be dye lasers pumped by either copper vapour or xenon chloride lasers.

job	file	date	report no.
16-529	819.39	March 16, 1987	87-60-K

TABLE OF CONTENTS

		Page
	Executive Summary	ii
1.	Introduction	1
2.	Fundamentals of Isotope Selective Photoionization	3
	a) Process Requirements	3
	b) Zirconium Ionization	3
	c) Zirconium Ground State Energy Levels	4
3.	Photoionization Schemes	5
	a) Search Procedure	5
	b) Copper Vapour Pumped Dye Lasers	5
	c) Xenon Chloride Pumped Dye Lasers	8
4.	Summary and Conclusions	9
Acknowledgements		10
References		11
Appendix A - Atomic Spectroscopy of Zirconium		12
Appendix B - ^{91}Zr Hyperfine Structure Constants		14
Figures		15

91601
new 82-10

ontario hydro
research division

EXECUTIVE SUMMARY

PHOTOIONIZATION SCHEMES FOR ATOMIC VAPOUR LASER ISOTOPE SEPARATION OF ZIRCONIUM

Hugh D. Morrison

Zirconium is used widely in the nuclear power industry and exclusively in CANDU reactors because of its low cross-section for thermal neutron absorption. Denaturing the isotopic composition of zirconium by depleting the ^{91}Zr isotope would result in a lower cross-section. Reactor components made of denatured zirconium would provide greater fuel burn-up through improved neutron economy. At the same time pressure tubes could be thicker, thereby extending their service lifetime. One technique that has been demonstrated for denaturing zirconium is atomic vapour laser isotope separation (AVLIS). In this method laser light is absorbed by selected zirconium atoms in a neutral atomic beam producing ions that are easily separated from the beam. The physics of the photoionization process depends on the spectroscopy of zirconium. High-resolution spectroscopy with tunable dye lasers reveals small isotope shifts in the transition wavelengths of zirconium but much larger shifts in ^{91}Zr due to its hyperfine structure. The hyperfine shifts are the key to zirconium isotope separation. This report examines the spectroscopic properties of atomic zirconium and the options they allow for photoionization schemes in zirconium AVLIS. Further investigation is proposed for several schemes that would employ dye lasers pumped by either copper vapour or xenon chloride lasers.

91601
new 82-10

ontario hydro
research division

To

Dr. D. Mills
Director of Research

PHOTOIONIZATION SCHEMES FOR ATOMIC VAPOUR LASER ISOTOPE SEPARATION OF ZIRCONIUM

Hugh D. Morrison

1. INTRODUCTION

Zirconium metal is vital to the nuclear power industry because of its low cross-section for thermal neutron absorption. This property combined with its good metallurgical properties makes zirconium almost ideal for nuclear reactor core components such as pressure tubes and calandria, and for the cladding of nuclear fuel bundles. Zirconium alloys are used exclusively for these components in CANDU reactors, the type of reactor used by Ontario Hydro. However, reactor operation could be improved if the thermal neutron absorption cross-section of zirconium in reactor components were reduced further. Of particular interest to Ontario Hydro is the possibility of increasing the thickness of pressure tubes to extend their service lifetimes without increasing, but perhaps decreasing, their neutron absorption. It has been recognized for many years that depleting or removing entirely one of the isotopes of zirconium would reduce its neutron cross-section. Zirconium has five isotopes of atomic mass 90, 91, 92, 94 and 96 (see Table 1). The mass 91 isotope has a natural abundance just over 11%, but it accounts for 75% of the thermal neutron absorption cross-section in natural zirconium. By reducing the concentration of ^{91}Zr to 3% the neutron cross-section of the denatured zirconium would be less than half that of the natural metal. The pressure tubes in Ontario Hydro's reactors are constructed with the Zr-2.5Nb alloy, zirconium with 2.5% niobium. Denaturing the zirconium in this alloy to the same extent would reduce the neutron cross-section by 45%, and would allow for an 80% increase in pressure tube thickness without increasing neutron absorption. The use of zirconium containing only 3% ^{91}Zr for all in-core components would provide greater flexibility in the design of nuclear reactors and that could result in longer service lifetimes, improved neutron economy and extended fuel cycles.

One of the methods that has been demonstrated to separate zirconium isotopes is atomic vapour laser isotope separation (AVLIS) performed with laser pumped tunable dye lasers. There are two reasons for continuing research and development into this method. The first is that zirconium AVLIS was demonstrated at the National Research Council of Canada (NRC)/1/. Thus there is an opportunity to develop a Canadian process for zirconium isotope separation that would benefit Canadian industry. The second reason is

TABLE 1

Zirconium Isotope Abundances and Neutron Cross-Sections

Mass Number	Natural Abundance (%)	Thermal Neutron Absorption Cross-section (mb)
90	51.46	14.4
91	11.23	1360
92	17.11	180
94	17.40	50
96	2.80	21
Natural Zirconium		200
Zirconium (3% 91)		96
Niobium		1339
Zr - 2.5 Nb		229
Zr (3% 91) - 2.5Nb		127

that the United States Department of Energy has selected AVLIS over several other advanced technologies for uranium isotope separation. Uranium and zirconium are sufficiently similar in physical and chemical properties that technology developed for uranium AVLIS could be applied to zirconium. Technology transfer would shorten the development time of a complete process for zirconium AVLIS.

There are three stages in AVLIS. The first stage involves generating the atomic vapour as a collimated beam from metal feedstock. In the second stage lasers are employed for isotope selective ionization of atoms in the beam by multi-step absorption of photons. In the final stage the ions are collected on charged plates flanking the atomic beam and the rest of the beam is collected on an end plate. Depending on which isotope has been

photoionized the denatured zirconium product will be either on the side plates or on the end plate. This report will examine the physics of several schemes for the photoionization process in the second stage and will also touch upon the requirements of an atomic vapour source for zirconium.

2. FUNDAMENTALS OF ISOTOPE SELECTIVE PHOTOIONIZATION

(a) Process Requirements

The technique of multi-step photoionization in AVLIS is illustrated in Figure 1 for both two and three step photon absorption. Ground state atoms are promoted to a first excited state by the absorption of photons at wavelength λ_{1a}, λ_{1b}, and λ_{1c}. The multiplicity of levels in the ground state is due to the fine structure of zirconium (see Section 2(c) and Appendix A). Isotope selectivity based on slight differences in the absorption wavelengths of the isotopes is most easily obtained in this first step. In zirconium, the isotope shifts are small compared to those in most other elements including uranium, but fortunately ^{91}Zr has a hyperfine structure that generates many hyperfine transitions with much larger wavelength shifts. The presence of hyperfine shifts in the one isotope that must be removed is both fortuitous and vital to the success of zirconium AVLIS. Subsequent photon absorption steps to reach the ionization potential must occur before the atoms relax to lower levels, as indicated by the lifetime τ_1 and by τ_2 for a second excited level in a three step scheme. The ease of exciting atoms up the energy ladder also depends on the cross-sections of the transitions. Knowledge of the ionization potential, energy levels and transitions, isotope and hyperfine shifts, absorption and ionization cross-sections, and level lifetimes is all required before a scheme of isotope selective photoionization can be chosen. A summary of the atomic spectroscopy of zirconium necessary for this discussion is provided in Appendix A.

One process factor of great economic importance is the quantity of laser energy expended per mole of denatured zirconium produced. Ionizing ^{91}Zr requires less than 10% as much energy per mole of product as compared to ionizing one or more even isotopes. In the former case ^{91}Zr is being removed and what is left in the atomic beam is the product, while in the latter case the product is being removed. Thus the search for a photoionization scheme is heavily weighted in favour of selectively ionizing ^{91}Zr. Economics also dictate that the final product must be obtained in a single pass from atom source to collector plates. This requirement translates into minimum acceptable limits on the efficiency of the photoionization and collection processes depending on the product desired and how it is obtained. The following discussion is based on a target level of 3% ^{91}Zr. This arbitrary level was chosen as a useful compromise between 6%, which would still be of use for pressure tubes, and 1%, which requires too much work to be economic.

(b) Zirconium Ionization

The ionization potential determines to some extent the type of lasers that can be used for photoionization. For zirconium, the ionization potential of 6.63 eV, or 53506 cm^{-1} /2/, means that three photons with an average wavelength of 560 nm or two photons with an average wavelength of 373 nm are required for photoionization. This means that copper vapour laser pumped dye lasers and most excimer laser pumped dye lasers are suitable for the task. The uranium AVLIS program employs copper vapour pumped dye lasers and

that technology is now well advanced. Of all the noble gas-halide excimer lasers, the xenon chloride laser has the highest output power of the chloride lasers and avoids the corrosion problems associated with the fluoride lasers. Xenon chloride pumped dye lasers were employed in the initial demonstration of zirconium AVLIS at NRC /1/.

(c) Zirconium Ground State Energy Levels

The transitions available for excitation in zirconium are affected by the characteristics of the vapour stream, so let us now examine how an atomic beam of zirconium would be produced. Zirconium is a refractory metal with a melting point of 2125 K and a boiling point of 4745 K /3/. The best method for generating a high throughput of atomic zirconium vapour is by vaporization with electron-beam heating. The fraction of vaporized atoms that remain in the vapour stream available to the lasers will depend on the geometry of the vapour source and of the stream with respect to the lasers. The vapour pressure of zirconium increases with temperature, and to produce pressures over 1 torr requires surface temperatures exceeding 3300 K /4/. At these temperatures many energy levels above the ground state in zirconium are highly populated. To provide access to as many zirconium atoms as possible for photoionization it is necessary to cool the internal electronic temperature of the atoms so that most of the population is in the ground state. The ground state configuration of zirconium, labelled a^3F, has a fine structure of three levels denoted by a^3F_J, where J is 2, 3 and 4, that lie at energies of 0, 570 and 1241 cm^{-1}, respectively. Figure 2 shows the fraction of the total population in these three levels as a function of electronic temperature up to 3000 K (derived from the energy level listing in Reference 3). The total fraction of zirconium atoms available in the ground state decreases with increasing electronic temperature as shown by the upper curve in Figure 3. Cooling a high temperature vapour stream down to 800 K by expanding the vapour would place over 99% of the atoms in the three ground state levels.

The lower curve in Figure 3 shows the sum of the population fraction in the two lower ground state levels a^3F_2 and a^3F_3. Accessing only these two levels would result in a simpler photoionization scheme at the expense of a lower fraction of zirconium atoms available unless the electronic temperature was less than 400 K. The available fraction directly affects the efficiency of the separation process no matter what isotope is ionized but the effect is most dramatic for ionizing ^{91}Zr since all atoms not ionized are collected on the end plate. Thus, to obtain less than 3% ^{91}Zr on the end plate in a ^{91}Zr photoionization scheme more than 75% of the ^{91}Zr atoms must be available for ionization. That fraction, indicated by the horizontal dashed line in Figure 3, also represents the minimum fraction of all the zirconium atoms that must be available for ionization in such a scheme. That requirement can be met by reducing the electronic temperature to less than 1500 K if only the two lower ground state levels are accessed, or to less than 3000 K if all three ground state levels are accessed. Obviously there is much more leeway for other process inefficiencies if all three levels are accessed and if the temperature is as low as possible.

3. PHOTOIONIZATION SCHEMES

(a) Search Procedure

The search for multi-step photoionization schemes can be limited somewhat by looking exclusively at schemes in which the first step of excitation from the ground state levels provides all the isotope selectivity and simultaneously leaves all the excited atoms in a common level for subsequent non-selective excitation to the ionization limit. These assumptions keep the scheme as simple as possible and minimize the consumption of laser energy by non-selective excitation. Furthermore, they recognize the practicalities of the experimental methods used to investigate photoionization schemes. Should more selectivity be required than the first step can provide then isotope selective excitation on subsequent steps can be investigated. The search for possible schemes is divided into two parts based on the pump lasers for the tunable dye lasers and then subdivided based on the alternatives provided by ionizing either ^{91}Zr or an even isotope and by accessing either two or three ground state levels. Thus, zirconium photoionization will be presented in terms of copper vapour pumped dye lasers first followed by a discussion of xenon chloride pumped dye lasers.

(b) Copper vapour pumped dye lasers

The copper vapour laser wavelength of interest here for pumping dye lasers is the 510 nm line which has produced dye lasers tunable from 564 to 688 nm /5/. With appropriate dyes this pump should be able to provide dye laser wavelengths tunable down to 535 nm. As no copper vapour lasers were available for the experiments described below other lasers were used to pump the tunable dye lasers.

The "allowed" transitions accessible to copper vapour pumped dye lasers from the ground state levels terminate in four levels, z^3F_2, z^3D_2, z^3F_3 and z^3D_3, and are listed in Table 2. Only the latter two levels can be reached from all three ground state levels. Four transitions to the first three of these levels have been examined by high-resolution laser fluorescence spectroscopy using a tunable dye laser with a line width of 7 MHz. Details of the experimental method are described in Reference 6. The sample spectra for these transitions, shown as Figures 4 to 7, all display a central cluster of four peaks due to the even isotopes surrounded by many smaller peaks due to the hyperfine splitting of ^{91}Zr. The even isotope peaks span about 500 MHz in frequency while the hyperfine structure can extend over 3 GHz. For each transition the hyperfine structure and isotope shifts have been measured and the hyperfine constants have been calculated for the z^3F_2, z^3F_3, and z^3D_2 levels (see Appendix B). Since hyperfine constants for the three ground state levels are known /7/ the hyperfine spectrum for any transition between the a^3F_J and the z^3F_2, z^3F_3, and z^3D_2 levels can be predicted. For the transitions not examined, the predicted hyperfine spectrum can be combined with an estimate of the even isotope spectrum to obtain a complete spectrum. The result is sufficient for determining the utility of the transition to isotope separation. Calculated spectra for the four measured transitions and the other three allowed transitions to the z^3F_2, z^3F_3, and z^3D_2 levels are shown as Figures 8 to 15. Figures 8 and 9 display the same transition with different vertical scales for comparing the relative heights of the even isotope peaks with the hyperfine peaks. The height of each even isotope peak and the sum of all the hyperfine peaks for ^{91}Zr is proportional to the abundance of the respective isotopes. With that normalization the heights of the hyperfine peaks are proportional to the strengths of the hyperfine transi-

TABLE 2

Optical Transitions (nm) from the Zirconium Ground State
Accessible to Copper Vapour Pumped Dye Lasers

Excited States	Ground States: a^3F_J		
	J=2	J=3	J=4
z^3F_2	613.6	635.9	---
z^3F_3	593.7	614.5	640.9
z^3D_2	561.4	579.9	---
z^3D_3	548.1	565.8	588.1

tions (see Appendix A). In Figures 9 to 15 the hyperfine transitions are labelled by the numerator of the hyperfine quantum number in their a^3F_J levels. The fractional populations of these hyperfine levels are listed in Table A in Appendix A. Knowing the populations is important in a ^{91}Zr photoionization scheme for exciting enough of the hyperfine transitions to achieve the depletion target.

The transitions to z^3F_2 and z^3D_2 are not suitable as the first step for photoionizing either ^{91}Zr or an even isotope because there are too many hyperfine peaks overlapping the even isotope peaks. The simplest looking spectrum, $z^3F_2 \leftarrow a^3F_2$ at 613.6 nm shown in Figure 9, illustrates this point. In this spectrum one group of hyperfine peaks lies in the shoulder of the ^{90}Zr peak and those components account for 27% of the ^{91}Zr. Thus there is no direct method of removing enough ^{91}Zr without throwing away a lot of ^{90}Zr. It would be possible to photoionize ^{92}Zr and ^{94}Zr without including too much ^{91}Zr, but that only applies to this one transition and not to $z^3F_2 \leftarrow a^3F_3$ (Figure 10) because of overlapping ^{91}Zr hyperfine peaks. As both transitions would be necessary for a viable separation scheme the first step excitation cannot terminate in z^3F_2. Similar arguments apply to the level z^3D_2 (Figures 11 and 12) which is also unsuitable as the common level in the first step.

The three transitions terminating in z^3F_3 (Figures 13 to 15) are all suitable for extracting ^{91}Zr because in each one the hyperfine components are grouped together so that one broad linewidth laser (~300 MHz linewidth) could excite enough hyperfine levels to achieve the required depletion. The lifetime of this level, 410 ns /8/, is many times longer than typical laser pumped dye laser pulses of 2-30 ns, and so presents no problem for a photoionization scheme. The transitions to z^3F_3 are not suitable for removing the even isotopes because those peaks are overlapped by too many hyperfine peaks.

The spectra of the transitions to z^3D_3 have not yet been examined but the level lifetime is 270 ns /9/. Hence this level could be useful if the hyperfine splitting is favourable. At least one transition to z^3D_3 should be probed to determine the hyperfine constants and then the spectra of the other two transitions can be predicted to assess their utility for isotope separation.

The steps to ionization after excitation to z^3F_3 or z^3D_3 can consist of either two visible photons from dye lasers in a three step process, or by a single uv photon in a two step process. A uv photon could be obtained either from an excimer laser (e.g. argon fluoride) or by frequency doubling the output of a copper vapour laser. Two-step photoionization is a simpler process but both options for doing so have disadvantages. Using an excimer laser in addition to a copper vapour pumped dye laser introduces a third type of laser and that will complicate the operation and maintenance of the separation process. Frequency doubling a copper laser does not have that disadvantage but frequency doublers are expensive relative to most other optics and inefficient at the copper laser wavelength. Both options for producing a uv photon have the disadvantage that their tuning range is limited to a few GHz. Tunability is as important for ionization as for other absorption steps because the cross-section for ionization varies with wavelength. Because of limited tunability the maximum cross-section available may be much less than the optimum.

An initial search for a second resonant step with a visible photon was conducted from the z^3F_3 level over the range 500 to 545 nm. This experiment required two dye lasers, one red laser tuned to 593.7 nm and a tunable green laser, to ionize the atoms in a three photon process. A strong transition was found at 520.19 nm with a resolution limited width of 0.02 nm and another weaker transition 0.2 nm wide was found at 544.15 nm. The first transition is well below the range available from copper vapour pumped dye lasers but it does tell us that there is an even parity level at 36068 cm^{-1}. The width of the second transition indicates two-photon ionization through an effective level rather than a resonance through a real level. The cross-section for this transition is much less than for the one at 520 nm and so may not be practical in a commercial photoionization scheme.

A similar scan of the green laser between 545 and 560 nm was performed with the red laser tuned to 579.9 nm to excite atoms to the z^3D_2 level. A strong transition was found at 547.8 nm and a weaker one at 552.8 nm. The second transition implies an even parity level at 35905 cm^{-1} to which no transition was found from 593.7 nm. By the rules for allowed transitions the quantum numbers of this level can be restricted to one of $^3D_1$, $^3P_2$, or $^3P_1$. The transition at 547.8 nm implies an even parity level at 36068 cm^{-1} which can be identified with the level found in the previous scan. Thus the quantum numbers of this level can be restricted to one of $^3D_2$, $^3D_3$, $^3F_2$, or $^3F_3$ which means that it should be accessible from the z^3D_3 level. This is significant because if the hyperfine shifts in the transitions to z^3D_3 provide sufficient isotope selectivity then the first two steps in a three step photoionization scheme will have been identified. Ionization in the third step will require photons at a wavelength less than 574 nm. At the moment this scheme represents the best chance for a copper vapour pumped dye laser system. The hyperfine shifts of z^3D_3 should be measured as soon as possible to confirm or reject the scheme.

(c) Xenon chloride pumped dye lasers

The xenon chloride excimer laser emits at 308 nm and has produced dye lasers tunable from 335 nm to 700 nm and beyond. This range includes all the wavelengths available from copper vapour pumped dye lasers. Thus all the schemes mentioned above could be obtained with XeCl pumped dye lasers. In addition, several new transitions in zirconium become accessible and simultaneously allow for two-step photoionization schemes where the second step is provided by a photon at 308 nm. Note that this case differs from the previous discussion of two-step photoionization in that the source of photons for the second step is already being used in the process and requires no extra optics. If attention is restricted to excited levels in zirconium with lifetimes much longer than 10 ns then only five levels remain of which only three are accessible from all three ground state levels. The five excited levels and the allowed transition wavelengths are listed in Table 3. The hyperfine structure and isotope shifts of these transitions need to be examined to assess their utility for isotope separation. Such experiments are planned for future work at NRC.

TABLE 3

Optical Transitions (nm) from the Zirconium Ground State
Accessible to Xenon Chloride Pumped Dye Lasers

Excited States	Ground States: a^3F_J		
	J=2	J=3	J=4
z^3G_3	457.7	469.9	485.2
y^3D_2	428.8	439.6	---
y^3D_3	422.6	433.1	446.0
y^3F_2	423.8	434.3	---
y^3F_3	424.3	434.8	447.9

4. SUMMARY AND CONCLUSIONS

There exists a need for denatured zirconium, zirconium depleted in ^{91}Zr, and an AVLIS process may prove to be a method for producing it in Canada. This report has examined details of the physics involved in the photoionization stage of AVLIS, wherein atoms from a vapour source are ionized selectively according to isotope by the absorption of light and then collected. The process economics dictate that sufficient separation must be achieved in a single pass and that it is preferable to ionize ^{91}Zr rather than any combination of even isotopes. Two well-developed laser technologies are suitable for photoionizing zirconium: copper vapour pumped dye lasers and xenon chloride pumped dye lasers. One difference between these laser systems is the range of wavelengths they can produce and hence the complexity they introduce into the overall process. Copper vapour pumped dye lasers require three photons to ionize a zirconium atom while xenon chloride pumped dye lasers can do the job with three or only two photons. The choice of laser system depends mostly on the wavelengths required for a complete photoionization scheme.

A desirable feature of any scheme is that the first step of excitation provide all the isotopic selectivity so that subsequent absorption steps to ionization can be non-selective. At once this keeps the scheme simple and minimizes the consumption of laser energy by non-selective excitation. In zirconium AVLIS, isotopic selective excitation must be applied to at least two of the three ground state levels, and possibly all three, depending on the electronic temperature of the atomic stream that reaches the lasers. To minimize the number of wavelengths required for a complete scheme, the first step must also leave all the atoms excited from the various initial levels in a common level. With these assumptions limiting the search, some potential schemes have been discovered and several rejected. The crucial test is isotope selectivity which in every case relies on the fact that the hyperfine shifts of ^{91}Zr greatly exceed the isotope shifts. However, none of the transitions examined are suitable for ionizing any one of the even isotopes because of interfering absorption by ^{91}Zr.

One complete three-step scheme employs the z^3F_3 level as the common level and requires xenon chloride pumped dye lasers to photoionize ^{91}Zr. Another three-step scheme, using copper vapour pumped dye lasers with the z^3D_3 level as the common level, will be successful for ionizing ^{91}Zr if the hyperfine shifts prove to be as favourable as those of z^3F_3. Both of these schemes access all three ground state levels. Another five schemes have been identified that rely on two-step photoionization from xenon chloride pumped dye lasers and three of these also access all the ground state levels. The utility of the two-step schemes cannot be fully assessed until their hyperfine structures and isotope shifts have been examined. There are plans for continued collaboration with NRC to answer some of these questions.

The existence of several possible photoionization schemes for zirconium AVLIS provides encouragement for more detailed research into the schemes and for closer examination of the economics of the whole process.

ACKNOWLEDGEMENTS

The experimental results described in this report were obtained in the laboratories of the Laser Chemistry Group headed by Dr. Peter Hackett at the National Research Council of Canada. I am grateful to Dr. Hackett, Dr. David Rayner and Dr. Orson Bourne for their collaboration in this venture.

Approved:

A.F. Baljet
Manager
Electrical Research Department

HDM/HDM/CB

Submitted:

H.D. Morrison
Engineering Physicist
Science Section
Electrical Research Department

REFERENCES

1. M.R. Humphries, O.L. Bourne and P.A. Hackett, "Laser isotope separation of zirconium atoms cooled in a supersonic beam", Chem. Phys. Lett. 118, 134 (1985).

2. P.A. Hackett, M.R. Humphries, S.A. Mitchell and D.M. Rayner, "The first ionization potential of zirconium atoms determined by two laser, field ionization spectroscopy of high lying Rydberg series", J. Chem. Phys. 85, 3194 (1986).

3. JANAF Thermochemical Tables, NSRDS-NBS37 (U.S. National Bureau of Standards, 1971).

4. R.K. Koch and W.E. Anable, "Vapor pressures of liquid molybdenum (2,890° to 2,990° K) and liquid zirconium (2,229° to 2795° K)", RI 7063 (U.S. Dept. of the Interior, Bureau of Mines, 1968).

5. R.S. Hargrove and T. Kan, "High power efficient dye amplifier pumped by copper vapor lasers", IEEE J. Quantum Electron. QE-16, 1108 (1980).

6. O.L. Bourne, M.R. Humphries, S.A. Mitchell and P.A. Hackett, "A high resolution laser induced fluorescence study of a supersonic zirconium atom beam", Opt. Commun. 56, 403 (1986).

7. S. Büttgenbach, R. Dicke, H. Gebauer, R. Kuhnen and F. Träber, "Hyperfine structure of seven atomic levels of ^{91}Zr and the ^{91}Zr nuclear electric quadrupole moment", Z. Physik A286, 125 (1978).

8. E. Biémont, N. Grevesse, P. Hannaford and R.M. Lowe, "Oscillator strengths for Zr I and Zr II and a new determination of the solar abundance of zirconium", Astrophys. J. 248, 867 (1981).

9. P. Hannaford and G.W. Series, "Observation of level-crossing effects in optogalvanic spectroscopy", J. Phys. B: At. Mol. Phys. 14, L661 (1981).

10. E.U. Condon and G.H. Shortley, The Theory of Atomic Spectra, p. 242, (Cambridge University Press, 1957).

APPENDIX A

Atomic Spectroscopy of Zirconium

The ground state term of atomic zirconium is labelled a^3F. This term denotes a particular configuration of the electrons about the nucleus and assumes that Russell-Saunders coupling of the electronic angular momentum vectors is valid. The capital F signifies that L = 3 where $\underline{L}$ is the total orbital angular momentum vector. The superscript 3 is the multiplicity of the state calculated from 2S+1 where $\underline{S}$ is the total electronic spin vector. The multiplicity is the number of levels of fine structure, labelled by J, that make up a state, and $\underline{J}$ is the vector sum of $\underline{L}$ and $\underline{S}$, the total angular momentum. Russell-Saunders coupling implies that L, S and J are all good quantum numbers. Thus, the ground state levels are denoted a^3F_J where J is 2, 3 and 4 obtained from $|L-S|$, $|L-S+1|$ and $|L-S+2| = |L+S|$. The prefix "a" in a^3F is an historical label for the lowest energy ^3F term. The fractional population of the a^3F_J levels depends on the partition function for all the fine structure levels defined by the level energies and the electronic temperature. The energies of the ground state levels J=2, 3 and 4 are 0.0, 570.41 and 1240.84 cm^{-1}, respectively. For comparison, the ionization potential is 53506.0 cm^{-1} on that scale, or 6.6339 eV/2/. The populations of these levels as a function of temperature are shown in Figure 2 of the main text.

Radiative transitions between levels are strongest for electromagnetic dipole-like transitions. The rules for "allowed" transitions of this type are defined in terms of changes in the values of L, S and J:

$$\Delta L = 0 \pm 1$$

$$\Delta S = 0$$

$$\Delta J = 0, \pm 1.$$

One final rule is that transitions are only "allowed" between levels of different parity. As the ground state has even parity, transitions from it must end in states of odd parity. States with odd parity are usually distinguished by a superscript "o" above the J value. In this report, the parity notation has been ignored and discussion has been limited to transitions that obey the parity rule.

The symbols for the values of L are:	S,	P,	D,	F,	G,	H, ...
for L =	0,	1,	2,	3,	4,	5, ...

Thus the allowed transitions from the a^3F_J levels end in levels labelled by ^3D, ^3F and ^3G with the appropriate values of J. Transitions to other states are observed but the cross-sections for allowed transitions are so much greater that other transitions have not been considered in the analysis of photoionization schemes.

For the odd isotope, ^{91}Zr, there is an additional level structure from a hyperfine interaction between $\underline{J}$ of the electrons and $\underline{I}$, the nuclear spin with I = 5/2. The vector sum of $\underline{J}$ and $\underline{I}$ is $\underline{F}$, and F can take the values $|J-I|$, $|J-I+1|$ and so on up to $|J+I|$. The tran-

sitions between hyperfine levels are governed by $\Delta F = 0, \pm 1$ in addition to the other transition rules. The energy of a hyperfine level, W_F, is given by the equation:

$$W_F = W_J + \frac{C}{2} A_J + \frac{3C(C+1) - 4I(I+1)\,J(J+1)}{8I(2I-1)\,J(2J-1)}$$

where $C = F(F+1) - I(I+1) - J(J+1)$.

W_J is the energy of the fine structure level, and A_J and B_J are Casimir constants, determined by experiment. Values of A and B for the ground state levels and for three excited levels are listed in Appendix B. The whole of the hyperfine splitting in any of the ground state levels spans less than 3 GHz (0.1 cm^{-1}). Thus the distribution of population within a hyperfine structure is not affected by the electronic temperature but only by the degeneracy of each level which is 2F+1. Table A shows the fractional population in the hyperfine levels expressed as a percentage of the population in their respective ground state levels.

The relative height of the hyperfine transition shown in Figures 8 to 15 are proportional to their transition strengths normalized to the natural abundance of ^{91}Zr with respect to the even isotope peak heights. That is, while the peak height of ^{96}Zr is given as 2.80, the sum of the heights of the hyperfine peaks is 11.23 (see Table 1 in main text). The relative transition strengths of the hyperfine components are determined by the angular momentum coupling coefficients. Tables of these values can be found, for example, in Reference 10.

Table A

Population Distribution (%) in the Hyperfine Structure of the Ground State Levels of ^{91}Zr

Ground States	Hyperfine Quantum Number, F						
	1/2	3/2	5/2	7/2	9/2	11/2	13/2
a^3F_2	6.7	13.3	20	26.7	33.3	-	-
a^3F_3	4.8	9.5	14.3	19.0	23.8	28.6	-
a^3F_4	-	7.4	11.1	14.8	18.5	22.2	25.9

APPENDIX B

^{91}Zr Hyperfine Structure Constants

The Casimir magnetic dipole (A) and electric quadrupole (B) factors for the hyperfine interaction in ^{91}Zr are listed below for the three ground state levels and for three excited levels. The ground state factors were obtained from Reference 7 and the excited state factors were calculated from scans of laser induced fluorescence spectroscopy described in this report and samples of which are shown in Figures 4 to 7. The number in parentheses following each value is the estimated error in the last digit.

Level	A (MHz)	B (MHz)
a^3F_2	-170.7696(38)	-21.500(29)
a^3F_3	-104.9441(38)	-24.187(49)
a^5F_4	-77.8878(38)	-33.476(62)
z^3F_2	-5(1)	0(10)
z^3F_3	-214(2)	-12(1)
z^3D_2	-180(5)	20(10)

FIGURES

Figure 1: Schematic diagram of photoionization process.

Figure 2: Population of ground state levels of zirconium as a function of temperature.

Figure 3: Zirconium fraction available for photoionization as a function of temperature.

Figure 4: Spectrum of zirconium at 613.6 nm.

Figure 5: Spectrum of zirconium at 579.9 nm.

Figure 6: Spectrum of zirconium at 593.7 nm.

Figure 7: Spectrum of zirconium at 614.5 nm.

Figure 8: Calculated spectrum of zirconium at 613.6 nm, full scale.

Figure 9: Calculated spectrum of zirconium at 613.6 nm.

Figure 10: Calculated spectrum of zirconium at 635.9 nm.

Figure 11: Calculated spectrum of zirconium at 561.4 nm.

Figure 12: Calculated spectrum of zirconium at 579.9 nm.

Figure 13: Calculated spectrum of zirconium at 593.7 nm.

Figure 14: Calculated spectrum of zirconium at 614.5 nm.

Figure 15: Calculated spectrum of zirconium at 640.9 nm.

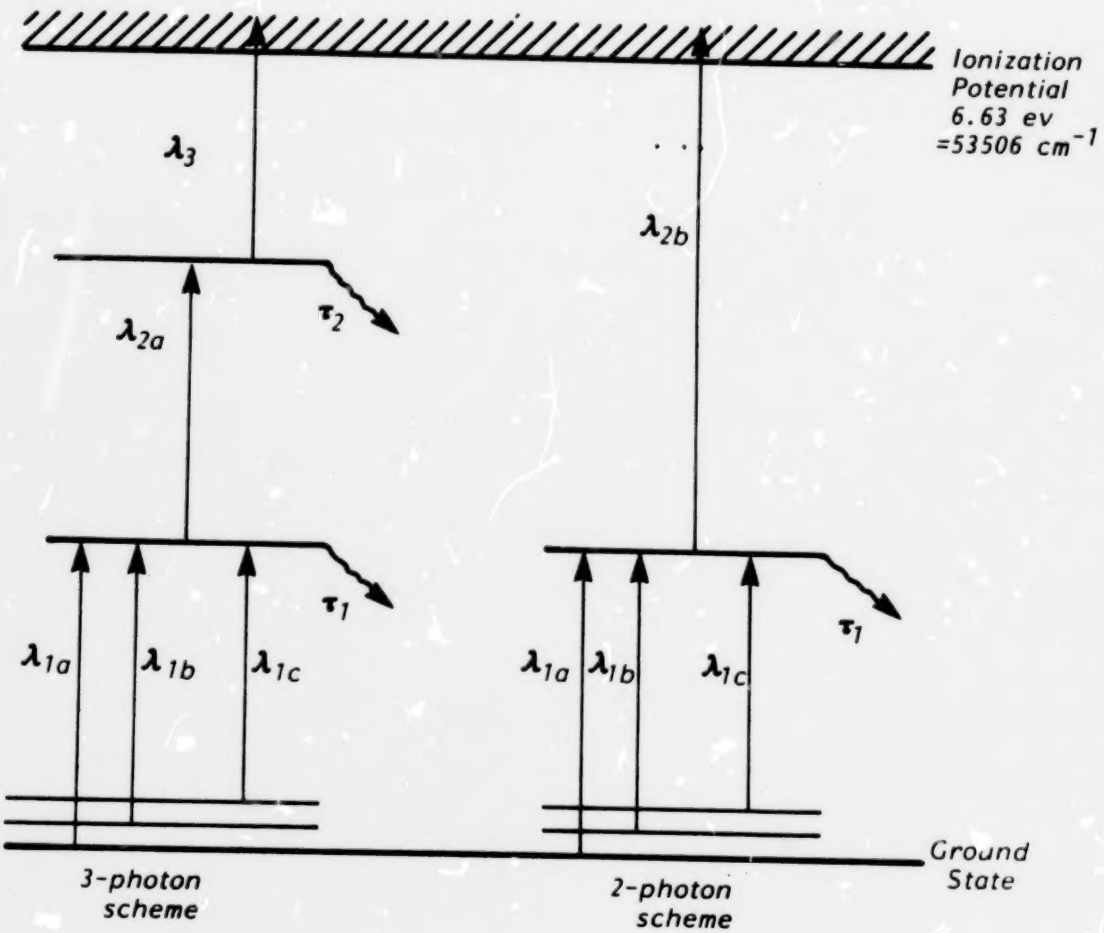

Figure 1: Schematic energy level diagram of zirconium illustrating two and three step photoionization from the three ground state levels. The transition wavelengths are indicated by λ and the level lifetimes by τ.

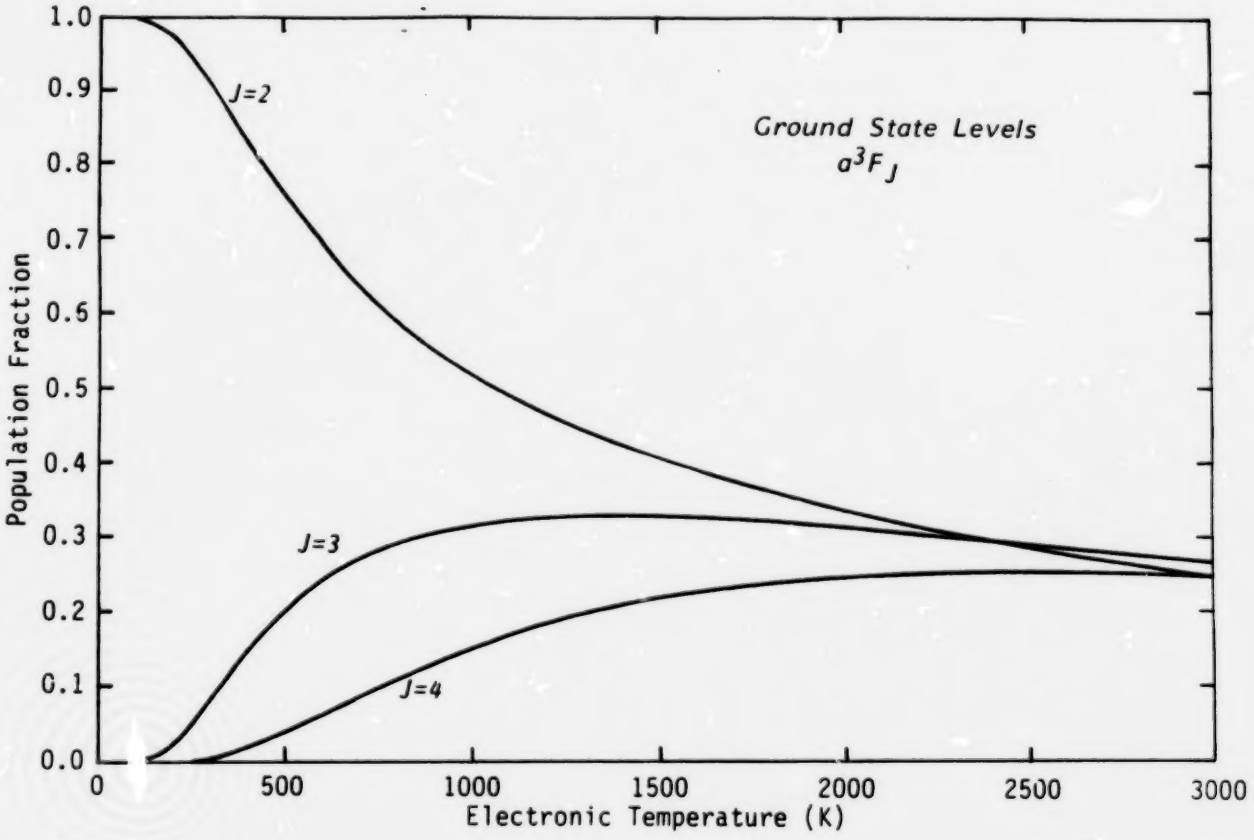

Figure 2: The relative populations of the three ground state levels of zirconium with respect to the total atomic population as a function of the electronic temperature.

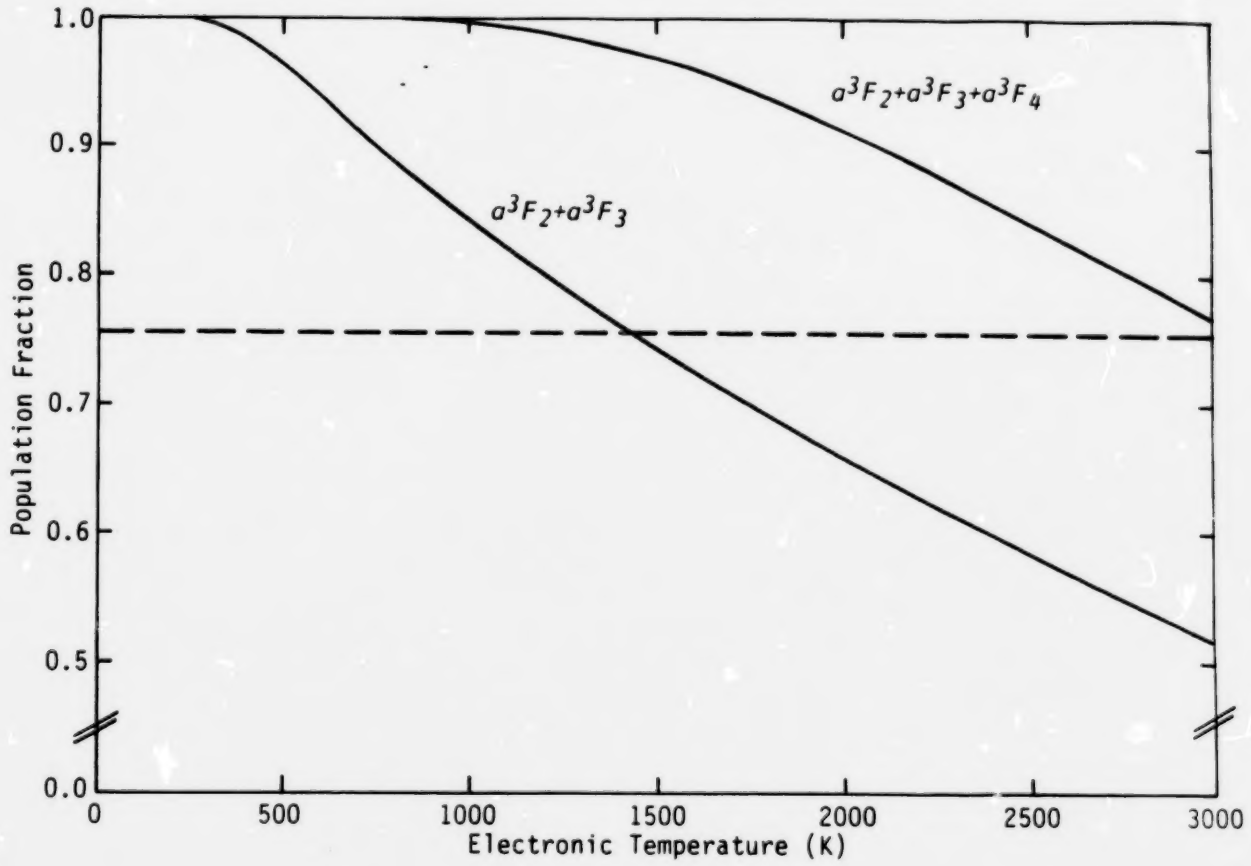

Figure 3: Total atomic zirconium population available for photoionization as a function of the electronic temperature when accessing all three ground state levels (upper curve) or only the lower two levels (lower curve). The minimum fraction needed to obtain 3% ^{91}Zr in the product stream of a ^{91}Zr photoionization scheme is given by the dashed horizontal line.

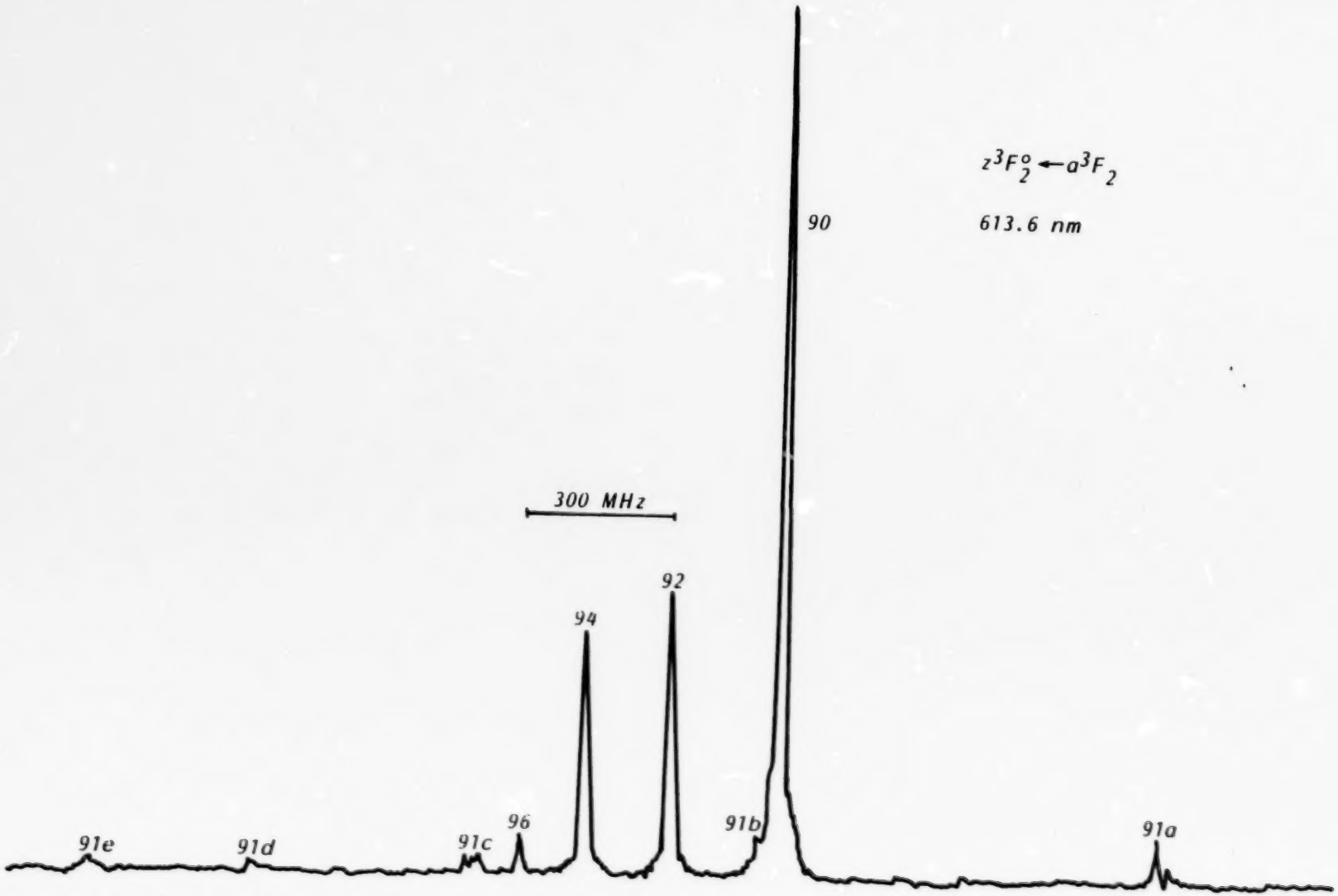

Figure 4: Laser induced fluorescence spectrum of zirconium at 613.6 nm resolving the peaks due to the even isotopes and to the hyperfine transitions of ^{91}Zr.

174269-RD

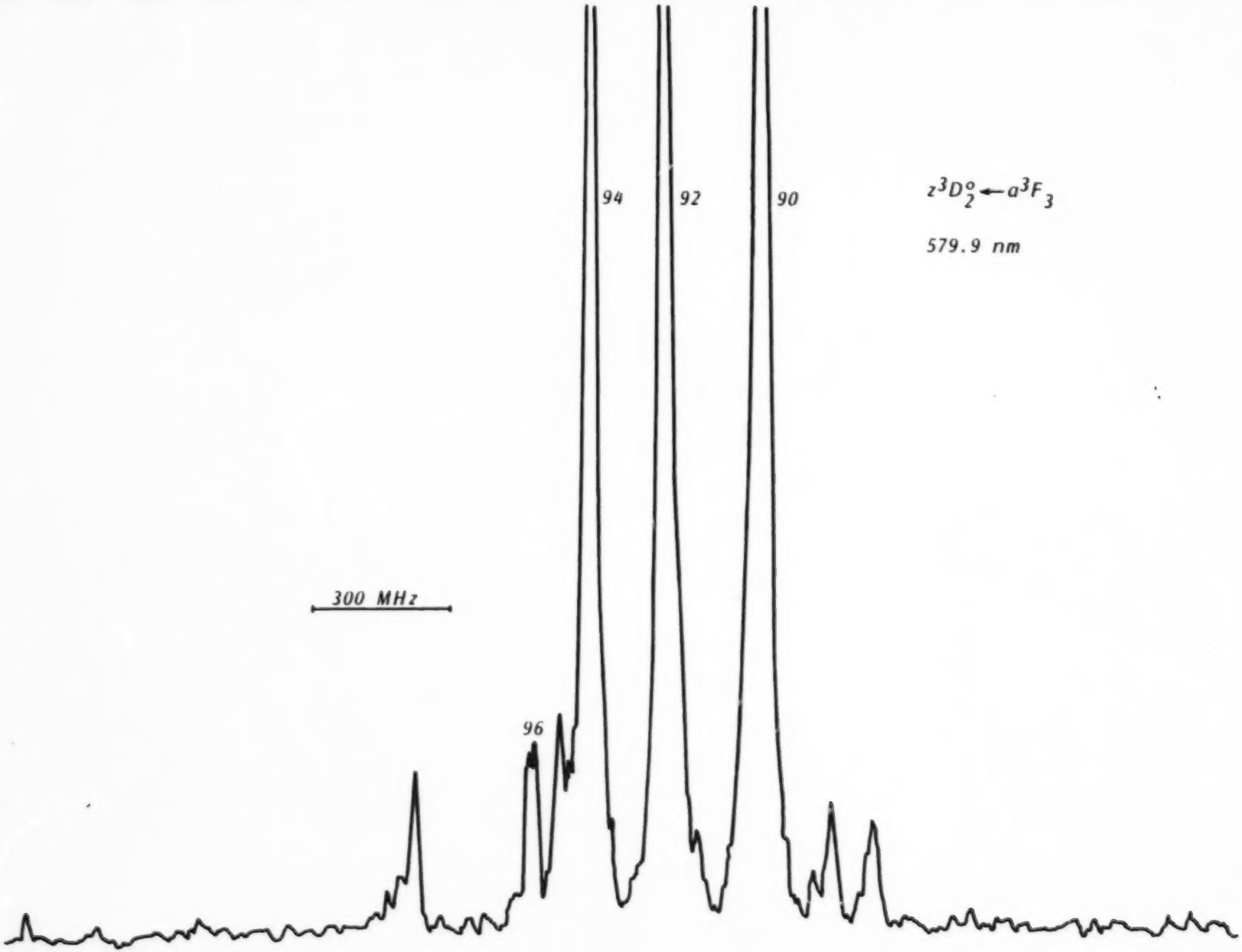

Figure 5: Laser induced fluorescence spectrum of zirconium at 579.9 nm resolving the peaks due to the even isotopes and to the hyperfine transitions of ^{91}Zr.

174270-RD

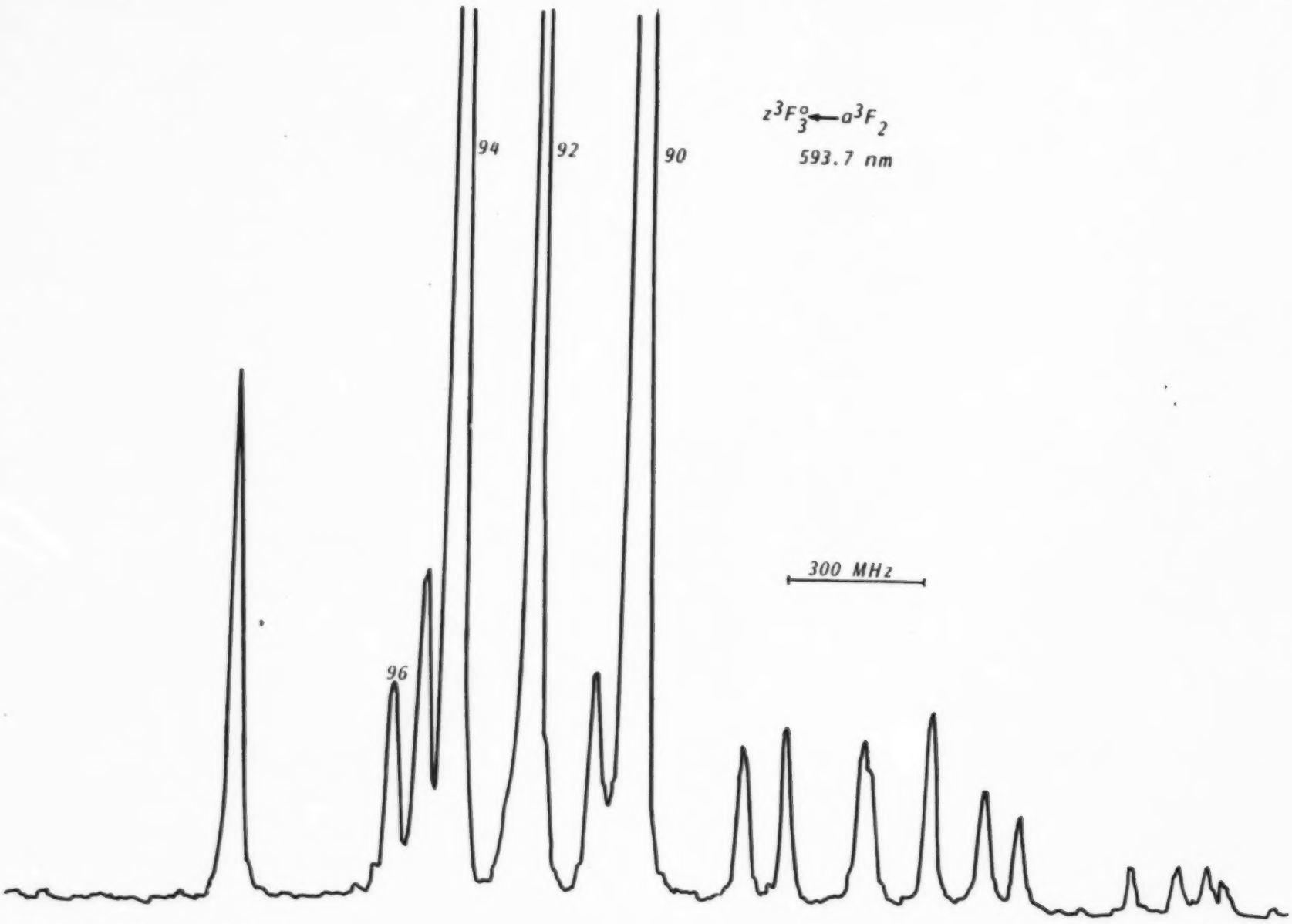

Figure 6: Laser induced fluorescence spectrum of zirconium at 593.7 nm resolving the peaks due to the even isotopes and to the hyperfine transitions of ^{91}Zr.

174271-RD

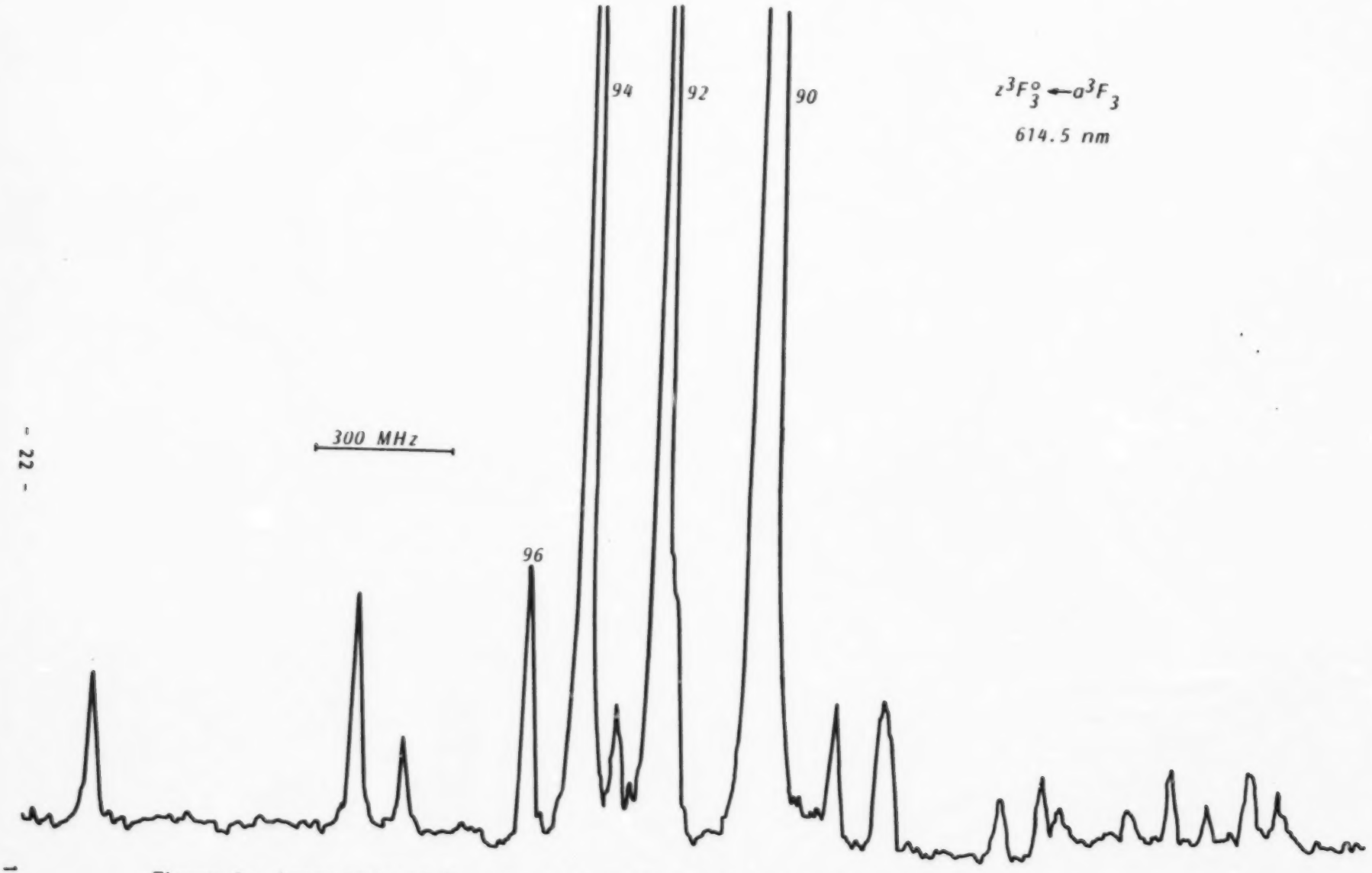

Figure 7: Laser induced fluorescence spectrum of zirconium at 614.5 nm resolving the peaks due to the even isotopes and to the hyperfine transitions of ^{91}Zr.

174272-RD

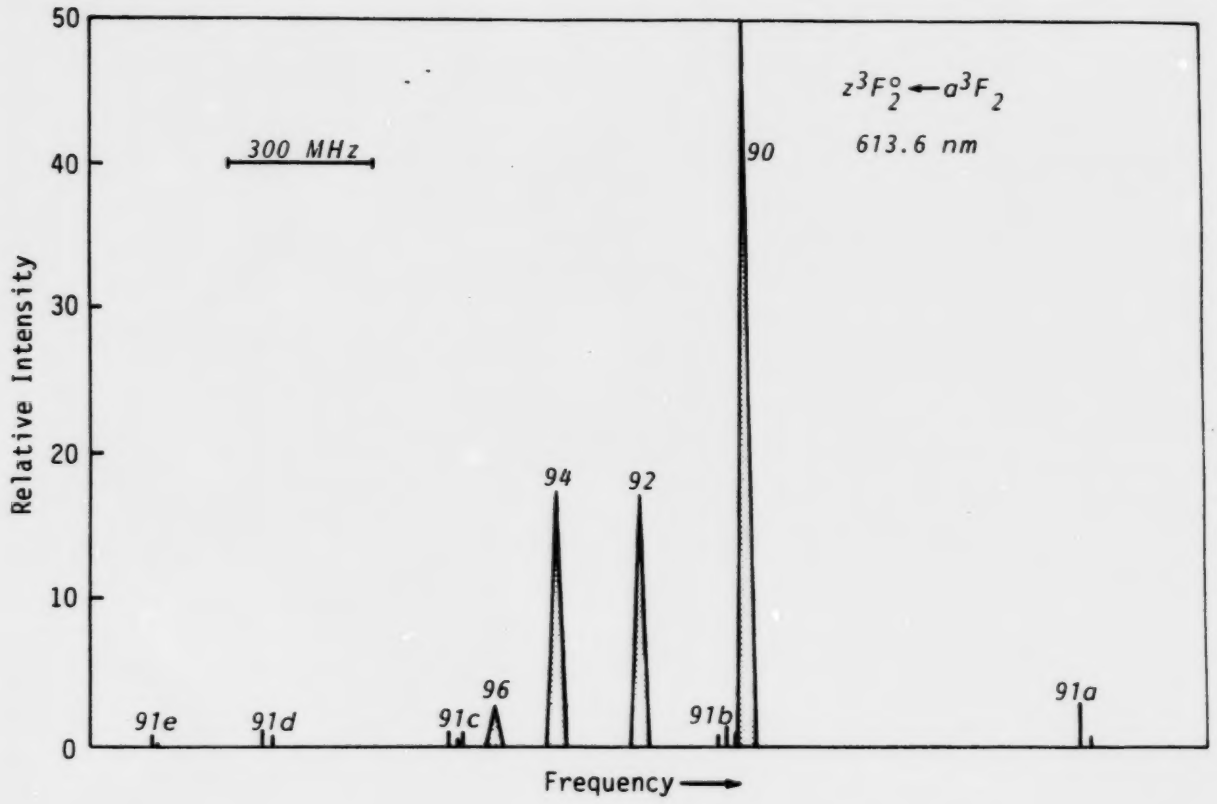

Figure 8: Calculated fluorescence spectrum of zirconium at 613.6 nm. The even isotope peaks are represented by shaded triangles while the hyperfine peaks of ^{91}Zr are represented by vertical lines.

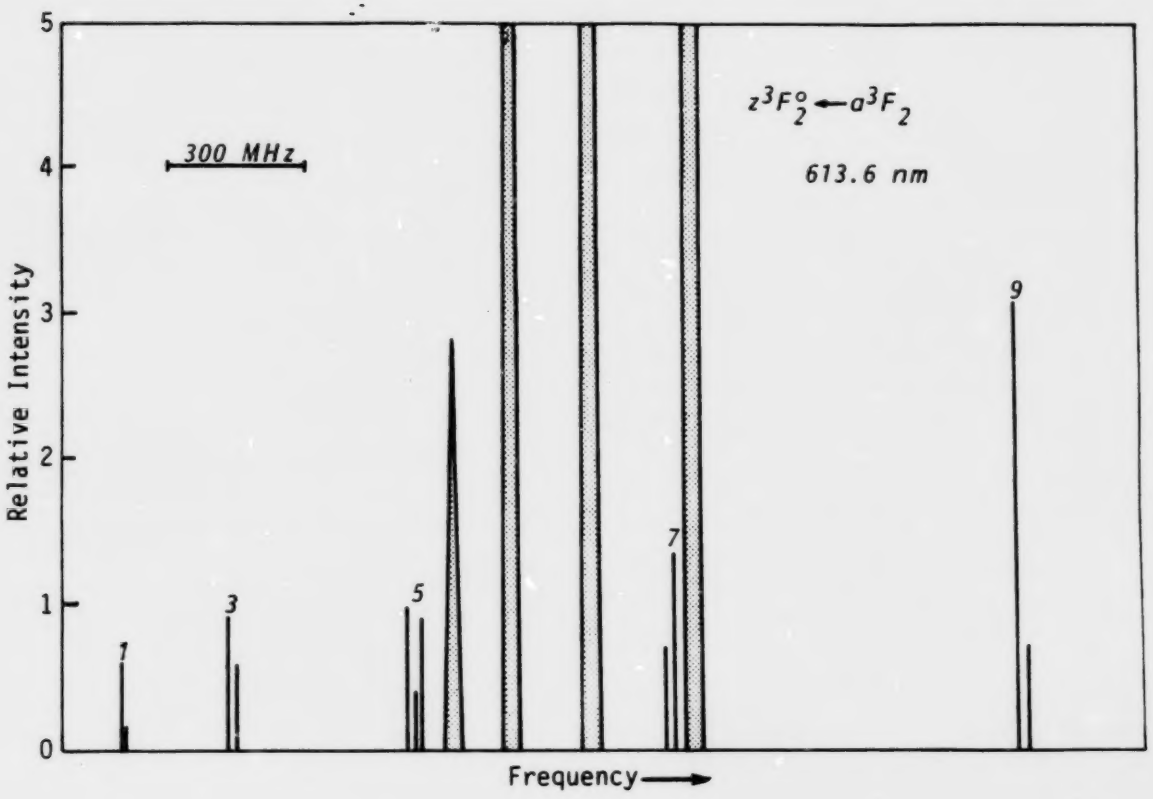

Figure 9: Calculated fluorescence spectrum of zirconium at 613.6 nm as in Fig. 8 but with an expanded vertical scale. Each ^{91}Zr hyperfine transition is identified by the numerator of the hyperfine quantum number in its lower level.

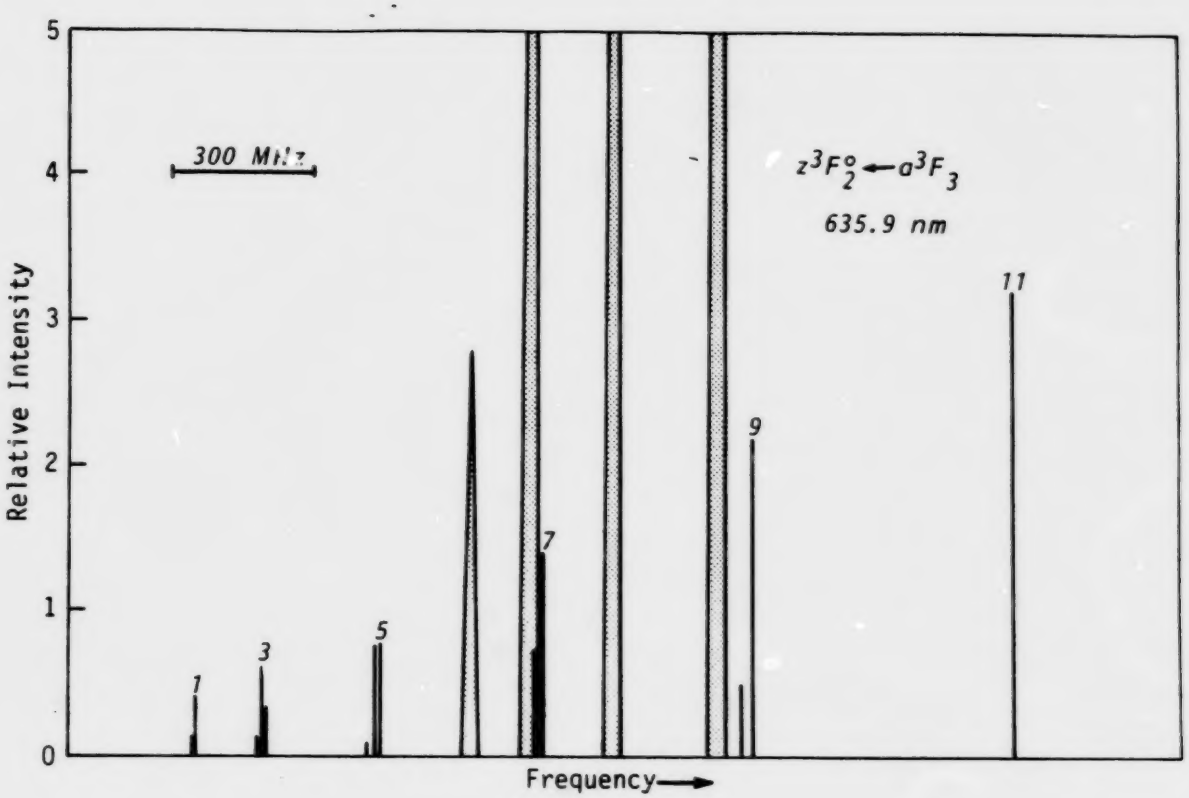

Figure 10: Calculated fluorescence spectrum of zirconium at 635.9 nm as in Fig. 9.

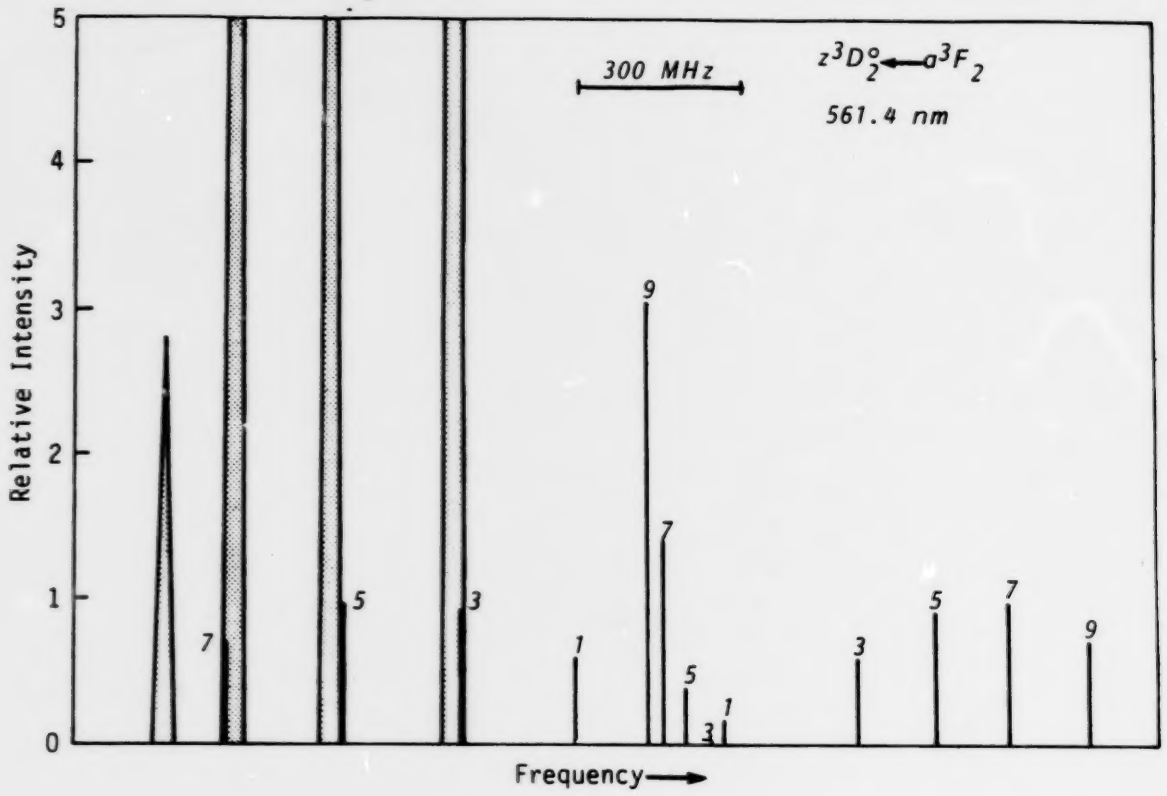

Figure 11: Calculated fluorescence spectrum of zirconium at 561.4 nm as in Fig. 9.

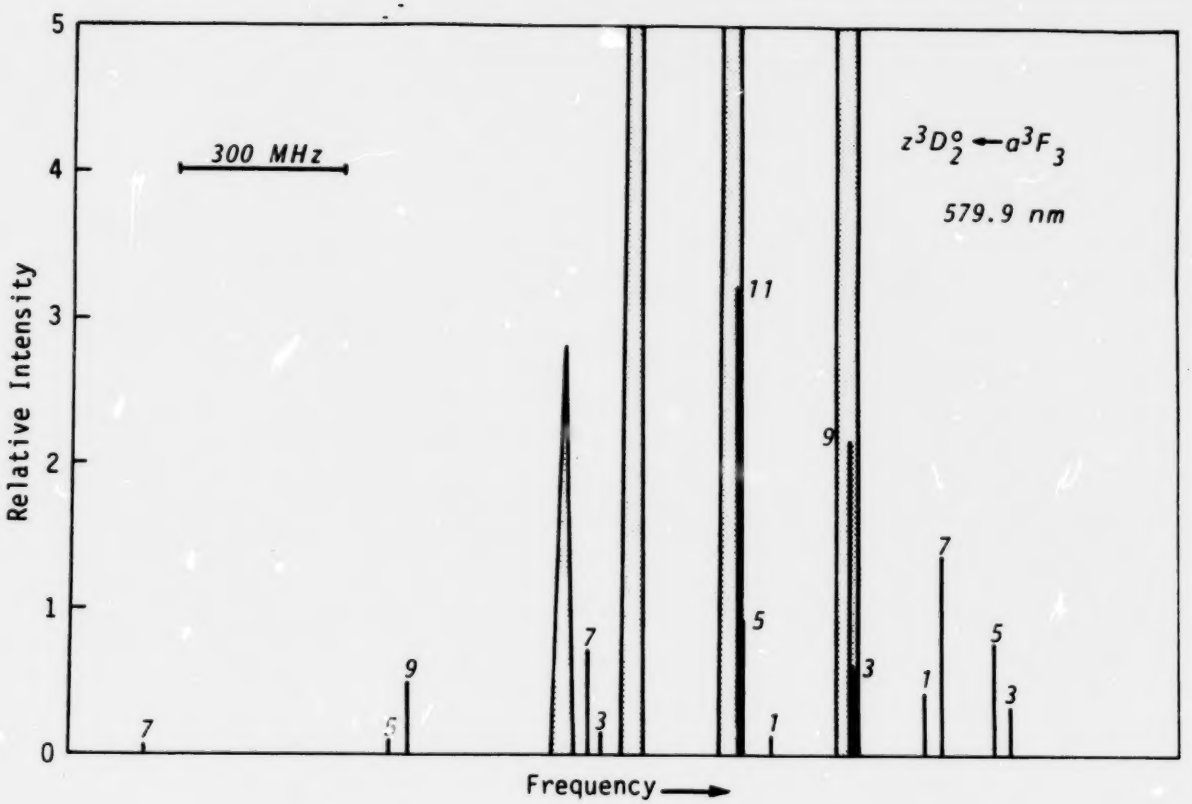

Figure 12: Calculated fluorescence spectrum of zirconium at 579.9 nm as in Fig. 9.

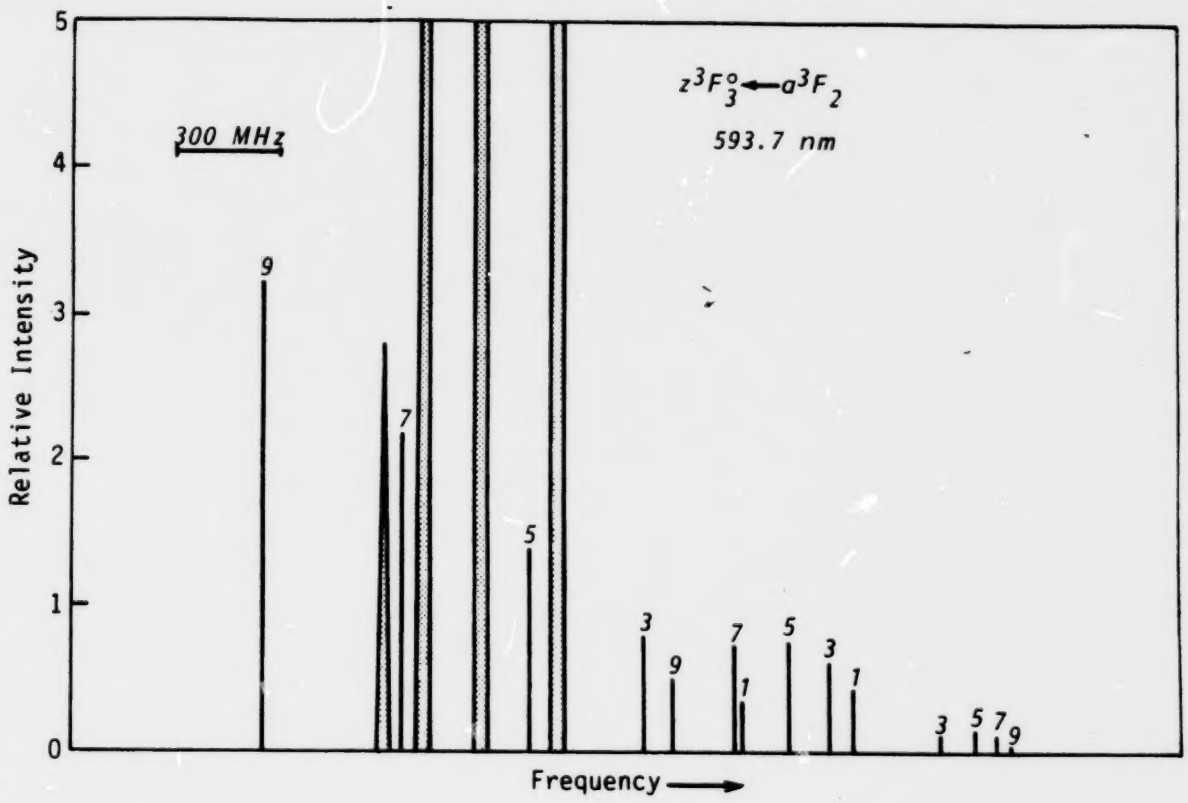

Figure 13: Calculated fluorescence spectrum of zirconium at 593.7 nm as in Fig. 9.

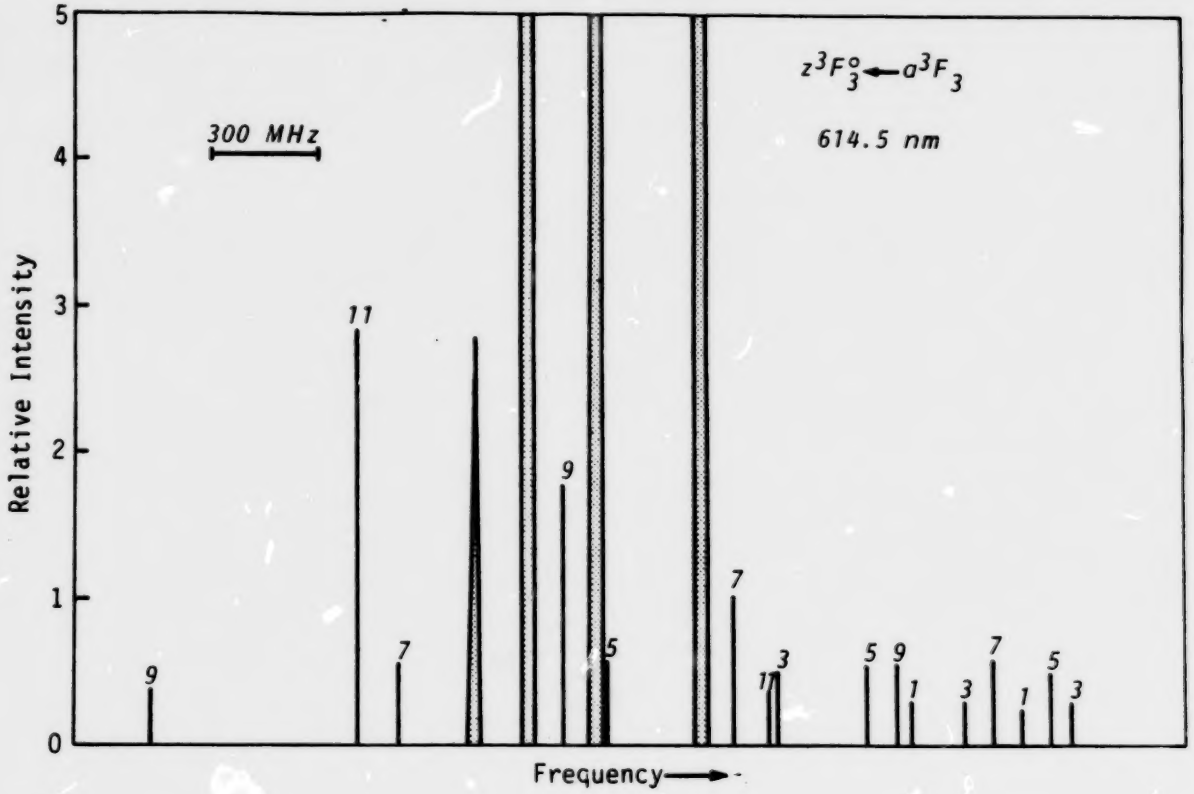

Figure 14: Calculated fluorescence spectrum of zirconium at 614.5 nm as in Fig. 9.

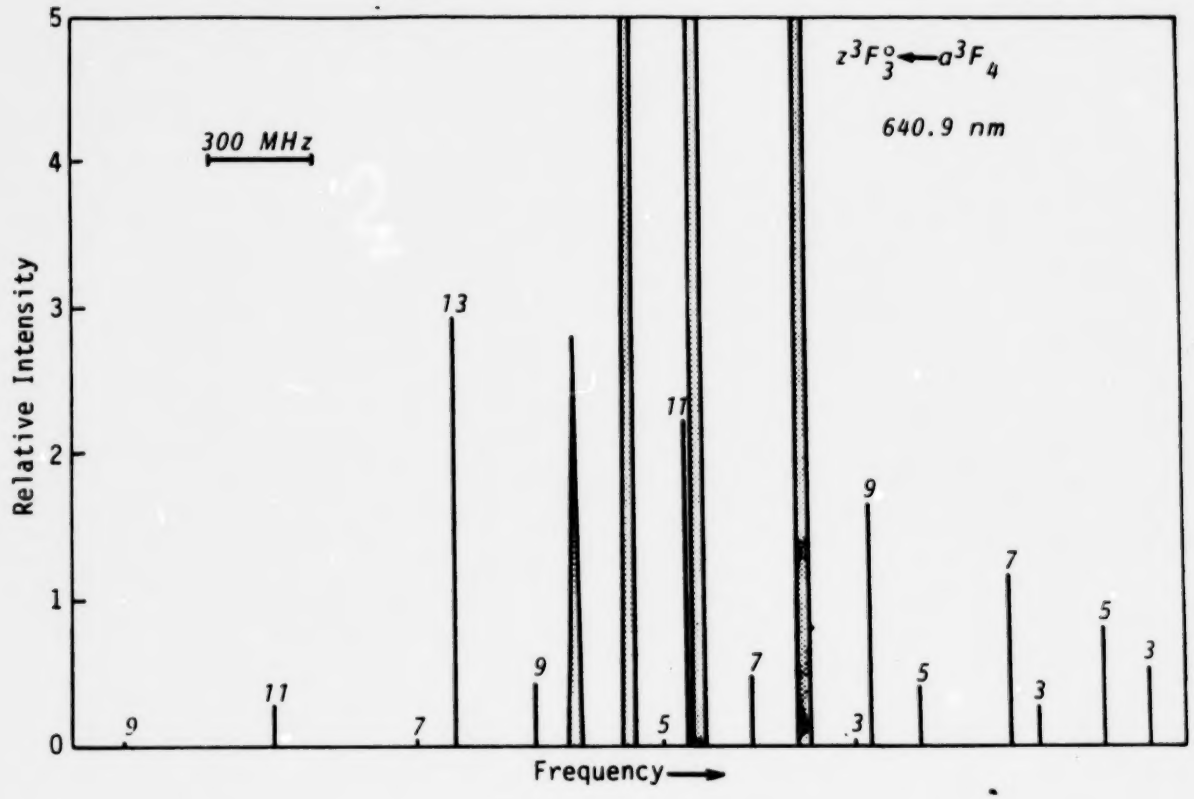

Figure 15: Calculated fluorescence spectrum of zirconium at 640.9 nm as in Fig. 9.

DISTRIBUTION

Dr. D. Mills	Director of Research
-- Dr. P.A. Hackett	National Research Council, Ottawa, Ontario
-- Dr. D.M. Rayner	National Research Council, Ottawa, Ontario
-- Dr. O.L. Bourne	National Research Council, Ottawa, Ontario
-- Mr. H.S. Irvine	Design & Development - Gen, H15A1
-- Mr. P.R. Burroughs	Design & Development - Gen, H15B01
-- Mr. H.N. Isaac	Design & Development - Gen, H11G27
-- Dr. R.A. Brown	Design & Development - Gen, H11A01
-- Mr. B.R. Collingwood	Design & Development - Gen, H15D02
-- Dr. G.J. Field	Design & Development - Gen, H10A16
-- Mr. T.J. Carter	Design & Development - Gen, H11A27
Dr. C.R. Frost	Design & Development - Gen, H11A26
Mr. R.A. McEachran	Design & Development - Gen, H11A27
-- Dr. G. Brenciaglia	Technical & Training Services, A7A13
-- Dr. P.T. Truant	Technical & Training Services, A7A10
-- Mr. E.G. Bazeley	Fuels, H06G01
Mr. A.F. Baljet	Research
Dr. C.J. Simpson	Research
Dr. P.C. Lichtenberger	Research
Dr. P. Mayer	Research
Dr. N. Anyas-Weiss	Research
Dr. K.B. Woodall	Research
Dr. J.R. Robins	Research
Dr. H.D. Morrison (2)	Research

Public Reference Centre
Editorial Section (2)
Office Copies (2)
Extra Copies (3)